
Title: Lysosomal permeabilization and endoplasmic reticulum stress mediate the apoptotic response induced after photoactivation of a lipophilic zinc(II) phthalocyanine

Authors: Nicolás Chiarante, María C. García Vior, Osvaldo Rey, Julieta Marino, Leonor P. Roguin

PII: S1357-2725(18)30177-8
DOI: https://doi.org/10.1016/j.biocel.2018.08.009
Reference: BC 5402

To appear in: *The International Journal of Biochemistry & Cell Biology*

Received date: 17-4-2018
Revised date: 6-8-2018
Accepted date: 15-8-2018

Please cite this article as: Chiarante N, García Vior MC, Rey O, Marino J, Roguin LP, Lysosomal permeabilization and endoplasmic reticulum stress mediate the apoptotic response induced after photoactivation of a lipophilic zinc(II) phthalocyanine, *International Journal of Biochemistry and Cell Biology* (2018), https://doi.org/10.1016/j.biocel.2018.08.009

# LYSOSOMAL PERMEABILIZATION AND ENDOPLASMIC RETICULUM STRESS MEDIATE THE APOPTOTIC RESPONSE INDUCED AFTER PHOTOACTIVATION OF A LIPOPHILIC ZINC(II) PHTHALOCYANINE

Nicolás Chiarante[a], María C. García Vior[a], Osvaldo Rey[b], Julieta Marino[a], Leonor P. Roguin[a*]

[a] Universidad de Buenos Aires, Consejo Nacional de Investigaciones Científicas y Técnicas, Instituto de Química y Fisicoquímica Biológicas (IQUIFIB), Facultad de Farmacia y Bioquímica, Junín 956, C1113AAD Buenos Aires, Argentina.

[b] Universidad de Buenos Aires, Consejo Nacional de Investigaciones Científicas y Técnicas, Instituto de Inmunología, Genética y Metabolismo (INIGEM), Facultad de Farmacia y Bioquímica, Córdoba 2351, C1120AAD Buenos Aires, Argentina.

* Corresponding author: Leonor Patricia Roguin. Instituto de Química y Fisicoquímica Biológicas (UBA-CONICET), Facultad de Farmacia y Bioquímica, Junín 956, C1113AAD Buenos Aires, Argentina. Tel.: +54 11 4964 8290; Fax: +54 11 4962 5457. E-mail: rvroguin@qb.ffyb.uba.ar

Graphical abstract

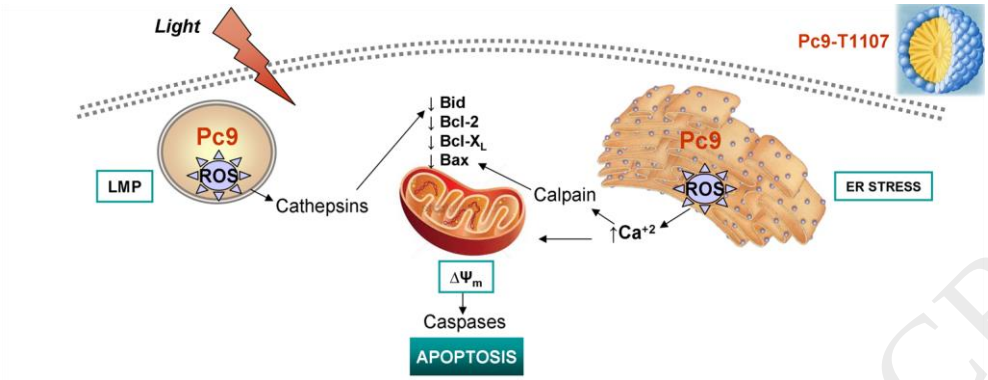


## Highlights

- We studied the apoptotic response activated by the lipophilic phthalocyanine Pc9

- Pc9 promotes lysosomal membrane permeabilization and induces ER stress

- Cathepsin D mediates Bid cleavage and caspase 8-activation

- Cytosolic $Ca^{2+}$ and calpains contribute to the apoptotic cell death program

- A model of Pc9-induced apoptotic pathways is proposed

**Abstract**

We have previously reported that the phototoxic action of the lipophilic phthalocyanine Pc9 (2,9(10),16(17),23(24) tetrakis[(2-dimethylamino)ethylsulfanyl]phthalocyaninatozinc(II)) encapsulated into poloxamine micelles is related to the induction of an apoptotic response in murine colon CT26 carcinoma cells. In the present study, we explored the intracellular signals contributing to the resulting apoptotic death. We found that Pc9-T1107 arrests cell cycle progression immediately after irradiation promoting then an apoptotic response. Thus, 3 h after irradiation the percentage of hypodiploid cells increased from 5.9 ± 0.6 % to 23.1 ± 0.1 %; activation of caspases 8 and 9 was evident; the population of cells with loss of mitochondrial membrane potential increased from 1.1 ± 0.4 % to 44.0 ± 9.3 %; the full-length forms of Bid and PARP-1 were cleaved; and a 50% decrease of the expression levels of the anti-apoptotic proteins Bcl-2 and Bcl-XL was detected. We also found that the photosensitizer, mainly retained in lysosomes and endoplasmic reticulum (ER), promotes the permeabilization of lysosomal membranes and induces ER stress. Lysosomal membrane permeabilization was demonstrated by the reduction of acridine orange lysosome fluorescence, the release of Cathepsin D into the cytosol and ~50% decrease of Hsp70, a chaperone recognized as a lysosomal stabilizer. Cathepsin D also contributed to Bid cleavage and caspase 8 activation. The oxidative damage to the ER induced an unfolded protein response characterized, 3 h after irradiation, by a 3-fold increase in cytosolic Ca2+ levels and 3 to 4 times higher expression of ER chaperones GRP78/BIP, calnexin, Hsp90 and Hsp110. The cell death signaling promoted by cytosolic $Ca^{2+}$, calpains and lysosomal proteases was partially abolished by the $Ca^{2+}$ chelator BAPTA-AM, the calpain inhibitor PD150606 and proteases inhibitors. Furthermore, Bax down-regulation observed in Pc9-treated cells was

undetectable in the presence of PD 150606, indicating that calpains contribute to Bax proteolytic damage. In summary, our results indicate that photoactivation of Pc9-T1107 led to lysosomal membrane permeabilization, induction of ER stress and activation of a caspase-dependent apoptotic cell death.

***Keywords:*** Photodynamic therapy; Phthalocyanine; Apoptosis; Lysosomal membrane permeabilization; ER stress; Calpains.

Abbreviations: Ac-LEHD-AMC, Ac-Leu-Glu-His-Asp 7-amino-4-methylcoumarin; BAPTA-AM, 1,2-Bis(2-aminophenoxy)ethane-N,N,N',N'-tetraacetic acid tetrakis(acetoxymethyl ester); CA-074 Me, (L-3-trans-(Propylcarbamoyl)oxirane-2-carbonyl)-L-isoleucyl-L-proline methyl ester; $DiOC_6(3)$, 3,3′-dihexyloxacarbocyanine iodide; ER, endoplasmic reticulum; PARP-1, poly-ADP-ribose-polymerase 1; Pc, phthalocyanine; PDT, photodynamic therapy; PD 150606, 3-(4-iodophenyl)-2-mercapto-(Z)-2-propenoic acid; PI, propidium iodide; PS, photosensitizer; ROS, reactive oxygen species; TROLOX, 6-hydroxy-2,5,7,8-tetramethylchroman-2-carboxylic acid; UPR, unfolded protein response; Z-IETD-AFC, Z-Ile-Glu-Thr-Asp 7-amido-4-trifluoromethylcoumarin.

## 1. Introduction

Colorectal cancer (CRC), the most common gastrointestinal malignant disease, represents the third most frequent type of cancer worldwide mainly affecting developed countries (Haggar et al., 2009; Kolligs, 2016; Favoriti et al., 2016; Doleman et al., 2016; Aran et al., 2016). Different strategies have been implemented to improve patient response and life expectancy (Patil et al., 2017), including the development of novel or combined therapies.

Photodynamic therapy (PDT) is an alternative and non-invasive approach for the treatment of a variety of cancers (Dougherty et al., 1998; Vicente, 2001; Detty et al., 2004; O'Connor et al., 2009; Dichiara et al., 2017). It basically consists in the administration of a photosensitizer (PS) that is activated by visible light in the presence of oxygen to produce reactive oxygen species (ROS). The cellular damage produced by these cytotoxic species is finally responsible to kill cancer cells. The cell death pathways triggered by PDT depend on the chemical nature and intracellular localization of the PS, the light doses employed and the genotype of the irradiated cells (Almeida et al., 2004; Buytaert et al., 2007; Moserova et al., 2012). Regardless of the molecular mechanism of death, the selective irradiation of cancer cells with minimal side effects represents an additional benefit of this therapeutic method. Among the different types of PS employed in PDT, the phthalocyanines (Pcs) have shown various advantages, such as the activation by wavelengths within the photo-therapeutic window (600-800 nm), allowing thus a deeper light tissue penetration, the efficient production of singlet oxygen and a low skin photosensitivity (Margaron et al., 1996; Colussi et al., 1999; Fabris et al., 2001; Taquet et al., 2007; Marino et al., 2010).

The endoplasmic reticulum (ER) is recognized as an essential organelle that maintains $Ca^{2+}$ homeostasis and is involved in post-translational modifications, folding and trafficking of new synthesized proteins. In addition, various studies have suggested an important role of the ER in the apoptotic process (Buytaert et al., 2007; Moserova et al., 2012). In this regard, stressful stimuli that affect protein synthesis or protein folding can activate a signaling network known as unfolded protein response (UPR) to restore ER homeostasis (Schröder et al., 2005; Szegezdi et al., 2006). The cell fate, in response to this activation, will depend on the ability to neutralize or not the stress, leading thus to cell survival or apoptosis.

We previously showed that the lipophilic phthalocyanine Pc9 (2,9(10),16(17),23(24) tetrakis[(2-dimethylamino)ethylsulfanyl]phthalocyaninatozinc(II)) encapsulated into Tetronic® 1107 polymeric poloxamine micelles exerted an effective phototoxic activity both in 2D and 3D cultures of murine colon carcinoma CT26 cells (Chiarante et al., 2017). We further demonstrated that after localizing into lysosome vesicles and ER cisterns, Pc9-T1107 promotes an apoptotic response (Chiarante et al., 2017). Herein, we explored the contribution of the intracellular signals triggered after PDT to the activation of an apoptotic program in colon cancer-derived cells. We found that, after photoactivation of Pc9-T1107, both the permeabilization of the lysosomal membrane and the induction of ER stress led to the activation of a mitochondrial-dependent pathway of apoptosis. The role of the released lysosomal proteases and the effect of the higher $Ca^{2+}$ levels found into the cytosol on the regulation of an apoptotic response were also investigated.

## 2. Materials and Methods

### *2.1. Chemicals*

Synthesis and purification of the sulfur-linked 2,9(10),16(17),23(24) tetrakis[(2-dimethylamino)ethylsulfanyl]phthalocyaninatozinc(II), named Pc9, has been previously described (O'Connor et al., 2009). Pepstatin A, PD 150606, monoclonal antibodies against Cathepsin D, Bax, and polyclonal anti-calnexin, anti-Hsp90, anti-actin, anti-PARP-1, anti-Bid, anti-Bcl-2 and anti-Bcl-$X_L$ antibodies were obtained from Santa Cruz Biotechnology (Santa Cruz, CA, USA). Monoclonal anti-Hsp70, anti-GRP78/BIP, anti-Hsp110 antibodies were obtained from Becton Dickinson (New Jersey, USA). Caspase substrates Z-IETD-AFC (caspase 8) and Ac-LEHD-AMC (caspase 9) were obtained from Peptide Institute Inc. (Osaka, Japan). Acridine orange, propidium iodide, the antioxidant 6-hydroxy-2,5,7,8-tetramethylchroman-2-carboxylic acid (TROLOX), aprotinin, BAPTA-AM and the fluorescent dye 3,3′-dihexyloxacarbocyanine iodide (DiOC6(3)) were obtained from Sigma Chemical (St. Louis, MO, USA). Fluo-4 AM was purchased from Invitrogen (Carlsbad, CA, USA). CA-074 Me was obtained from Enzo Life Sciences. Poloxamine Tetronic® 1107 (T1107, MW 15 kDa) was a gift from BASF (Germany).

### *2.2. Cells and culture conditions*

Murine colon carcinoma CT26 cells (ATCC CRL-2638) were maintained in RPMI-1640 (Gibco BRL) containing 10% (v/v) fetal bovine serum (FBS, Gibco BRL), 2 mM L-glutamine, 50 U/mL penicillin and 50 mg/mL streptomycin, in a humidified atmosphere of 5% $CO_2$ at 37 ºC.

*2.3. Photodynamic treatment*

CT26 cells were plated in 96-well microplates at a density of 2 x $10^4$ cells/well in RPMI-1640 supplemented with 10% FBS and incubated overnight at 37 °C until 70-80% of confluence. Then, culture medium was replaced by RPMI-1640 containing 4% FBS with or without different concentrations of Pc9-T1107. After 24 h, cells were exposed to a light dose of 2.8 J $cm^{-2}$, 1.17 mW $cm^{-2}$, with a 150 W halogen lamp equipped with a 10 mm water filter to maintain cells cool and attenuate IR radiation. In addition, a cut-off filter was used to bar wavelengths shorter than 630 nm, as described previously (O'Connor et al., 2009). After irradiation, cells were incubated for an additional 24 h period and cell number was evaluated by the MTT reduction assay. In some experiments, cells were pre-incubated 1 h or 24 h before irradiation with different concentrations of specific protease inhibitors (Pepstatin A, CA-074 Me or aprotinin), a calcium chelator (BAPTA-AM) or a calpains inhibitor (PD 150606).

*2.4. Cell cycle analysis*

CT26 cells were incubated for 24 h in the presence or absence of 20 nM Pc9-T1107 at 37 °C. After irradiation (2.8 J $cm^{-2}$), cells were incubated for different time periods, trypsinized and washed with cold PBS. 1 x $10^6$ cells were fixed overnight with 1 mL of 70% cold ethanol and kept at 4 °C. Cells were washed twice with PBS and resuspended in 500 µL of 0.1% sodium citrate, 0.1% Triton X-100, 50 µg/mL propidium iodide (PI), pH 7.5. After incubating overnight at 4 °C, cell cycle phase distribution was assessed in a BD Accuri cell cytometer (BD Biosciences, CA, USA).

*2.5. Flow cytometry DNA analysis*

To evaluate the proportion of hypodiploid cells, approximately 1 x $10^6$ CT26 cells were incubated for 24 h with or without 20 nM of Pc9-T1107 at 37 °C. After irradiation, cells were incubated for different time periods and treated as described above. The hypodiploid DNA content was then analyzed in a BD Accuri cell cytometer.

*2.6. Caspase activity assay*

After incubating CT26 cells for 24 h with 20 nM Pc9-T1107, cells were washed, irradiated with a light dose of 2.8 J $cm^{-2}$ and incubated for different time-periods at 37 ºC. 1 x $10^7$ cells were then lysed for 30 min at 4 ºC in 50 µL of lysis buffer (10 mM HEPES, pH 7.4, 50 mM NaCl, 2 mM $MgCl_2$, 5 mM EGTA, 1 mM PMSF, 2 µg/mL leupeptin, 2 µg/mL aprotinin) followed by three cycles of rapid freezing and thawing. Cell lysates were centrifuged at 17,000 x g for 15 min and total protein concentration was determined using Bradford reagent. Aliquots containing 100 µg of protein were diluted in assay buffer (20 mM HEPES, 132 mM NaCl, 6 mM KCl, 1 mM $MgSO_4$, 1.2 mM $K_2HPO_4$, pH 7.4, 20% glycerol, 5 mM DTT), and incubated at 37 °C for 1 h with 50 µM of the corresponding fluorogenic substrate for caspase 8 (Z-IETD-AFC) and caspase 9 (Ac-LEHD-AMC). Cleavage of the substrates was monitored by AMC or AFC release in a SFM25 Konton Fluorometer at 355 or 400 nm excitation and 460 or 505 nm emission wavelengths, respectively. In some experiments, cells were pre-incubated for 1 h with 80 µM of Pepstatin A before irradiation.

*2.7. Western blot assays*

CT26 cells were incubated for 24 h with 10 nM or 20 nM of Pc9-T1107, then washed with PBS and exposed to a light dose of 2.8 J $cm^{-2}$. After irradiation, suspensions containing 1 x $10^6$ cells were immediately lysed for 30 min at 4 ºC in 10 µL of lysis buffer (0.5% Triton

X-100, 1 µg/mL aprotinin, 1 µg/mL trypsin inhibitor, 1 µg/mL leupeptin, 10 mM $Na_4P_2O_7$, 10 mM NaF, 1 mM $Na_3VO_4$, 1 mM EDTA, 1 mM PMSF, 150 mM NaCl, 50 mM Tris, pH 7.4). Alternatively, irradiated cells were incubated for different times at 37 ºC and cell lysates were prepared. In some experiments, cells were pre-incubated before irradiation for 24 h with 100 µM of the calpain inhibitor PD 150606 or for 1 h with 80 µM of Pepstatin A, and cell lysates were prepared 1 h after irradiation. Clear supernatants were obtained after centrifugation at 17,000 x g for 10 min at 4 ºC and protein concentration was determined using Bradford reagent. Aliquots containing 50 µg of protein were resuspended in 0.063 M Tris/HCl, pH 6.8, 2% SDS, 10% glycerol, 0.05% bromophenol blue, 5% 2-ME, submitted to SDS-PAGE and then transferred onto PVDF membranes (GE Healthcare, Piscataway, NY) for 1 h at 100 V in 25 mM Tris, 195 mM glycine, 20% methanol, pH 8.2. After blocking with 10 mM Tris, 130 mM NaCl and 0.05% Tween 20, pH 7.4, containing 3% bovine serum albumin (BSA), membranes were treated as the usual western blotting method. The applied secondary antibodies anti-mouse IgG (horseradish peroxidase-conjugated goat IgG) or anti-rabbit IgG (horseradish peroxidase-conjugated goat IgG) were from Santa Cruz Biotechnology, CA, USA. Immunoreactive proteins were visualized using the ECL detection system (Amersham Biosciences, Piscataway, NY) according to the manufacturer´s instructions. For quantification of band intensity, Western blots were scanned using a densitometer (Gel Pro Analyzer 4.0). Equal protein loading was confirmed by reprobing membranes with rabbit anti-actin (Sigma-Aldrich, Inc., Missouri, USA) or muose anti-tubulin antibodies (Abcam, Cambridge, UK).

*2.8. Evaluation of mitochondrial membrane potential*

In order to measure $\Delta\Psi_m$, CT26 cells pre-loaded with or without 20 nM Pc9-T1107 for 24 h in the dark at 37 ºC were treated with a light dose of 2.8 J $cm^{-2}$. Immediately after irradiation or 1-3 h later, cells were incubated with 40 nM of the potential-sensitive cationic lipophilic dye 3,3′-dihexyloxacarbocyanine iodide (DiOC6(3)) for 30 min at 37 °C. Green fluorescence for DiOC6(3) was measured by using a BD Accuri cell cytometer.

*2.9. Lysosomal stability assessment*

CT26 cells were grown on coverslips and incubated in the presence or absence of 20 nM Pc9-T1107 for 24 h at 37 ºC in the dark. After photodynamic treatment with 2.8 J $cm^{-2}$, cells were incubated for different time periods and stained with acridine orange (5 µM, 30 min, 37 ºC) to label lysosomes (Boya et al., 2003). In some experiments, cells were pre-incubated for 1 h before irradiation with 5 mM of the antioxidant TROLOX and stained 1 h after irradiation. Cells were examined with a fluorescence Olympus BX50 microscope with the corresponding filter, 470-490 nm excitation and 515 nm emission wavelengths.

*2.10. Subcellular fractionation and immunodetection of Cathepsin D*

After incubating CT26 cells for 24 h in the presence or absence of 20 nM Pc9-T1107, cells were washed with PBS and exposed to a light dose of 2.8 J $cm^{-2}$. Then, cells were incubated for different time-periods at 37 °C and for the detection of Cathepsin D suspensions containing $2 \times 10^6$ cells were washed twice with sucrose buffer (250 mM sucrose, 20 mM HEPES, pH 7.5, 10 mM KCl, 1.5 mM $MgCl_2$, 1 mM EDTA, 1 mM EGTA, 1 mM DTT, 0.1 mM PMSF, 1 µg/mL aprotinin, 1 µg/mL leupeptin), resuspended in 20 µL of sucrose buffer and incubated on ice for 15 min. Cells were then homogenized with a Dounce (40 strokes) and centrifuged at 1,000 × g for 10 min at 4 °C. The resulting supernatant

was centrifuged at 20,000 × g for 20 min at 4 °C, and final supernatants (50 µg of protein/lane) were loaded onto a SDS-PAGE, transferred onto PVDF membranes and revealed with an anti-Cathepsin D antibody. Quantification of band intensities was performed by using a densitometer (Gel Pro Analyzer 4.0). Actin was employed as loading control of cytosolic fraction.

*2.11. Measurement of intracellular $Ca^{+2}$ levels*

To evaluate intracellular $Ca^{+2}$ levels, CT26 cells (2 x $10^4$/well) were grown in culture medium supplemented with 10% FBS and incubated overnight at 37 ºC until 70-80% of confluence. Complete culture medium was then replaced by medium containing 4% FBS with or without different concentrations of Pc9-T1107. After incubating cells for 24 h, cells were washed with PBS, incubated with 2 µM of Fluo-4 AM for 30 minutes at 37 °C and then irradiated with a light dose of 2.8 J $cm^{-2}$. In some experiments, cells were pre-incubated for 1 h before irradiation with a 5 mM concentration of the antioxidant TROLOX. Fluorescence intensity values were determined with a FlexStation 3 microplate reader (Molecular Devices Inc., USA) at 494 nm excitation and 516 nm emission wavelengths.

*2.12. Statistical analysis*

The values are expressed as mean ± S.E.M of three different experiments. Statistical analysis of the data was performed by using one way analysis of variance (ANOVA) followed by Dunnett or Bonferroni post-hoc test where appropriate. $p<0.05$ denotes a statistically significant difference.

**3. Results**

*3.1. Pc9-T1107 treatment arrests cell cycle and regulates mitochondrial apoptosis*

We have previously showed that the photoactivation of the lipophilic phthalocyanine Pc9 encapsulated into T1107 polymeric micelles induced a caspase 3-dependent apoptotic cell death both in 2D and 3D cultures of colon carcinoma CT26 cells (Chiarante et al., 2017). In order to characterize the cascade of intracellular events leading to cell photodamage, we first examined cell cycle phase distribution after incubating CT26 cells pre-loaded with a 20 nM concentration of Pc9-T1107 for different times after irradiation (Fig. 1A). Immediately after light exposure, Pc9-T1107 treatment caused a significant decrease of the percentage of cells in $G_0/G_1$ and an increase in the population of cells in S and $G_2$/M phases (Fig. 1A). This effect on cell cycle phases was maintained for at least 5 h post-irradiation (p.i.) (Fig. 1A). At longer incubation times, the time-dependent increment in the percentage of hypodiploid cells obtained after irradiation of Pc9-treated cells avoided the study of cell cycle phases. The induction of an apoptotic cell death was then evaluated by determining the sub-$G_1$ fraction of CT26 cells by flow cytometry. Histograms shown in Fig. 1B revealed that the population of hypodiploid cells, representing an apoptotic state, increased at 3 h and 24 h post-irradiation. Since we previously reported the enzymatic activation of the executioner caspase 3 after irradiation of CT26 cells loaded with Pc9-T1107 (Chiarante et al., 2017), we next examined whether caspases 8 and 9 also participate in the phototoxic action induced by the photosensitizer. Results shown in Fig. 1C revealed a similar increase of caspase 8 activity at 1 h, 3 h and 24 h post-irradiation, whereas a significant increase of caspase 9 activity was evident after 3 h and 24 h, indicating that both initiator caspases would be involved in caspase 3 activation.

To further characterize the apoptotic response induced by Pc9-T1107, we examined the expression levels of several members of the Bcl-2 family of proteins. As shown in Fig. 2A, a marked down-regulation of the anti-apoptotic proteins Bcl-$X_L$ and Bcl-2 was observed immediately after irradiation (0 h p.i.), an effect that lasted for at least 3 h. It was also detected an almost complete loss of Bid, suggesting the cleavage of the full-length form to the truncated pro-apoptotic tBid (Kaufmann et al., 2001). Noticeably, the proteolytic cleavage of the pro-apoptotic Bax protein was also detected as a result of Pc9-T1107 photoactivation, being Bax levels reduced immediately after irradiation (Fig. 2A). In addition, the cleavage of PARP-1, a caspase 3-substrate that plays a role in DNA repair (Rodríguez-Hernández et al., 2006; Hassa et al., 2008) was also evident 3 h after irradiation of Pc9-loaded cells (Fig. 2A).

The involvement of the mitochondrial pathway was next studied by determining the mitochondrial membrane potential ($\Delta\Psi_m$) with the DiOC6(3) green fluorescent probe. Results shown in Fig. 2B revealed that the population of cells with loss of membrane potential increased immediately at 0 h p.i. (26.6 ± 11.9 % versus 1.1 ± 0.4 %, control cells) and even more 1-3 h after light exposure (51.0 ± 9.7 % and 44.0 ± 9.3 %, respectively).

*3.2. Pc9-T1107 affects lysosomal membrane stability*

In a previous study, we demonstrated that Pc9-T1107 localizes mainly into lysosomal vesicles and ER cisterns in CT26 cells and that Pc9-T1107 induced the generation of ROS immediately after cell irradiation (Chiarante et al., 2017). In order to gain a better understanding of the molecular mechanisms mediating the cell death by Pc9-T1107, we examined the biological effects triggered by ROS formation in the intracellular organelles retaining Pc9-T1107. When CT26 cells were stained with acridine orange, a dye that is

trapped within acidic organelles such as lysosomes, a remarkable decrease of the fluorescence was immediately observed after irradiation, suggesting the partial permeabilization of the lysosomal membrane (Fig. 3A). To further corroborate this observation, the cells were incubated in the presence of 5 mM TROLOX, an antioxidant concentration previously reported to protect cells from the phototoxic effect of Pc9-T1107 (Chiarante et al., 2017). As shown in Fig. 3 B, no loss of acridine orange fluorescence was detected, suggesting that ROS generated upon irradiation contribute to alter the integrity of lysosomal membranes. In addition, the approximately 2.5-fold increase in the cytosolic levels of the lysosomal enzyme cathepsin D observed 1-3 h after irradiation also indicated the destabilization or partial permeabilization of the lysosomal membrane (Fig. 3C). We further evaluated the expression levels of the heat shock protein 70 (Hsp70), a molecular chaperone that has been involved in maintaining the integrity of lysosomal membranes (Nylandsted et al., 2004; Doulias et al., 2007; Petersen et al., 2010). The almost 50% reduction of Hsp70 levels determined at different times after light exposure also supported the conclusion that Pc9-T1107 photoactivation promotes the permeabilization of the lysosomal membrane (Fig. 3D).

Based on these findings, we next evaluated the effect of different proteases inhibitors on cell survival. Thus, it has been reported that Pepstatin A inhibits various aspartic proteases that reside in the lysosomes, including Cathepsin D (Johansson et al., 2003; Heinrich et al., 2004; Liaudet-Coopman et al., 2006), whereas CA-074 Me behaves as a Cathepsin B inhibitor (Cho et al., 2013; Victor et al., 2011). A significant increase in cell survival was observed after irradiation of Pc9-loaded CT26 cells pre-incubated 1 h before light exposure with 80 μM Pepstatin A or 1 μM CA-074 Me (Fig. 4A and B). Similar results were observed when the cultures were pre-incubated with aprotinin, a serine protease inhibitor (Dobkowski

et al., 1998; Peters et al., 1999), suggesting that besides cathepsins D and B, other proteolytic enzymes contribute to the phototoxic action mediated by Pc9-T1107 (Fig. 4C). In addition, since it has been described that Cathepsin D released in a ROS-dependent manner can activate caspase 8 (Conus et al., 2008; Marino et al., 2013), we evaluated the contribution of this protease to the apoptotic pathway by determining caspase 8 activity in the presence or absence of Pepstatin A. Results shown in Fig. 4D revealed a significant reduction of caspase 8 activity after light exposure of Pc9-CT26 cells pre-incubated with the Cathepsin D inhibitor. Furthermore, it has also been reported that Cathepsin D and other lysosomal proteases can be involved in the cleavage of Bid to generate tBid, a truncated form of this protein involved in the permeabilization of the mitochondrial outer membrane (Stoka et al., 2001; Reiners et al., 2002; Droga-Mazovec et al., 2008). When the expression levels of Bid were determined in the presence of 80 μM of Pepstatin A, a noticeable recovery of the amount of full length Bid was evident at 1 h p.i., indicating a role for Cathepsin D in Bid activation (Fig. 4E).

*3.3. Pc9-T1107 triggers endoplasmic reticulum stress*

The intracellular localization of Pc9 in the ER led us to evaluate whether the local generation of ROS could activate the ER stress response referred to as unfolded protein response (UPR). To examine the role of ER stress in the apoptotic response induced by Pc9-T1107, the expression of several UPR-related proteins was determined at different times after irradiation of Pc9-treated CT26 cells. Results obtained by Western blot revealed a significant increment of the expression levels of the ER chaperones GRP78/BIP, calnexin and heat shock proteins (Hsp) 90 and 110, at 3 h p.i. (Fig. 5A). In addition, as part of the stress response, we further explored the influence of PDT treatment on the release of $Ca^{2+}$ into the cytosol. A

dose- and time-dependent increase in cytosolic $Ca^{2+}$ was determined at different times after irradiation of CT26 cells loaded with $IC_{50}$ or $2xIC_{50}$ of Pc9-T1107 (Fig. 5B). When CT26 cells exposed to $2xIC_{50}$ of Pc9-T1107 were pre-incubated with a 5 mM concentration of the antioxidant TROLOX, a reduction in the intracellular $Ca^{2+}$ concentration obtained at 3 h p.i. was evident, suggesting the involvement of ROS in the deregulation of $Ca^{2+}$ levels (Fig. 5C). The influence of $Ca^{2+}$ as a mediator of death signals was then assessed by using the $Ca^{2+}$ chelator BAPTA-AM. As shown in Fig. 5D, the antiproliferative action promoted by 2 nM of Pc9-T1107 was partially reversed in the presence of BAPTA-AM, indicating a role for $Ca^{2+}$ in the mechanism of cell death.

Because the activation of the $Ca^{2+}$-dependent cysteine proteases calpains has been extensively reported during ER stress (Dougherty et al., 1998; Moserova et al., 2012), we then decided to test the effect of the calpain inhibitor PD 150606 (Pollack et al., 2003) on cell viability. After incubating Pc9-T1107-treated cells with different concentrations of PD 150606, a significant increment of cell survival was observed at 50-100 μM inhibitor concentrations, indicating that calpains are also involved in the cell death program triggered by Pc9-T1107 (Fig. 6A). Based on this result, we inquired if the calpains could play a role in the down-regulation of Bax levels observed after PDT treatment. In this regard, we found an almost complete recovery of Bax expression levels after PDT of Pc9-CT26 cells pre-incubated with a 100 μM concentration of PD 150606 (Fig. 6B), revealing that calpains are indeed mediating Bax proteolytic damage.

## 4. Discussion

We previously reported that the lipophilic phthalocyanine Pc9 is a potent PS that induces a rapid apoptotic response in colon carcinoma-derived cells. Several lines of independent evidence presented here reveal that multiple intracellular pathways mediate Pc9-pro-apoptotic mechanisms of cell death. Specifically, our results show that Pc9 induced a cell cycle arrest characterized by a shift in the population of cells in S and $G_2$/M phases. The increase in the sub-$G_1$ population of cells observed at later times post-irradiation reinforced that an apoptotic response is associated to the PS antiproliferative effect. The contribution of cell cycle arrest and apoptosis in PDT-induced tumour cell death has been previously reported for other PS, although it is known that the effect on cell cycle distribution is dependent on the chemical nature of the PS and the cell line tested. Thus, besides inducing an apoptotic death, cell cycle arrest in $G_1$ phase has been reported for a tetra-triethyleneoxysulfonyl substituted zinc phthalocyanine in gastrointestinal cancer cells (Kuzyniak et al., 2016), and an S phase arrest was observed in response to PDT with a phenylporphyrin derivative in lung carcinoma cells (Liu et al., 2015; Wang et al., 2015).

Pc9 treatment was also associated to several typical features of apoptosis (Kaufmann et al., 2001; Hengartner, 2000; Galluzzi et al., 2012), including activation of caspases 8 and 9, loss of mitochondrial membrane potential, activation of Bid, the decrease of the anti-apoptotic proteins Bcl-2 and Bcl-$X_L$ and PARP-1 cleavage. After identifying the apoptotic cell death triggered by PDT, we examined the role of lysosomes and ER, the organelles that retain the photosensitizer and therefore represent the main sites that initiate the cascade of molecular signals leading to cell photodamage (Buytaert et al., 2007;Olinick et al., 2002; Chiu et al., 2010). It has been reported that the peroxidation of membrane lipids favoured by ROS formation can alter the integrity of lysosomal membranes (Roberg et al., 1999; Repnik

et al., 2012; Kågedal et al., 2001). Our data showed that the loss of the acridine orange fluorescence observed after irradiation of Pc9-loaded CT26 cells was reversed in the presence of TROLOX, suggesting the mediation of ROS in the destabilization of lysosomal membranes. This result was supported by the increment in cytosolic Cathepsin D, a lysosomal enzyme involved in the regulation of an apoptotic response (Repnik et al., 2012; Guicciardi et al., 2004; Johansson et al., 2010; Boya et al., 2008). We also observed, as a result of Pc9 photoactivation, a down-regulation of Hsp70, a lysosomal stabilizer that inhibits membrane permeabilization (Nylandsted et al., 2004; Doulias et al., 2007; Petersen et al., 2010). Consistent with our findings, the contribution of lysosomal membrane permeabilization to the apoptotic death induced after PDT has been previously described for other lysosome-targeted photosensitizers, such as a cationic zinc(II) phthalocyanine (Marino et al., 2013), chlorin e6 formulations (Reiners et al., 2002; Li et al., 2016), and the porphyrin derivative ATX-s10 (Ichinose et al., 2006), among others.

Lysosomal enzymes released into the cytosol appear to play a role as mediators of apoptosis through the digestion of critical intracellular proteins (Repnik et al., 2012; Johansson et al., 2010; Boya et al., 2008). In this study, the contribution of lysosomal enzymes to cell death was first supported by the increase in cell survival observed after pre-incubating Pc9-loaded CT26 cells with different proteolytic inhibitors. We next showed that the activation of caspase 8 induced after PDT was significantly inhibited in the presence of Pepstatin A, suggesting that Cathepsin D behaved as an upstream regulator of caspase 8 activation. A Cathepsin-dependent activation of caspase 8 has been previously reported in the apoptosis induced both in neutrophils (Conus et al., 2008) and some cancer-derived cells (Jancekova et al., 2016; Lin et al., 2016). We also showed that Cathepsin D inhibition increases the full length protein Bid, indicating a role of this lysosomal protease in Bid

degradation and activation, in a similar way to that reported by other authors after PDT (Stoka et al., 2001; Reiners et al., 2002; Droga-Mazovec et al., 2008; Appelqvist et al., 2012). In summary, Cathepsin D actively participates in the mechanism of Pc9-induced CT26 cell death by altering the levels of apoptotic intracellular signals.

We further evaluated the involvement of an ER stress response after Pc9-T1107 photodynamic treatment of CT26 cells. The endoplasmic reticulum is an organelle that exerts an important role in protein synthesis, folding and trafficking, and functions as calcium storage within the cell. Among the different insults that can disturb ER homeostasis, we inquired whether Pc9 incorporated into ER cisterns could cause stress and activate an UPR after PDT. While ER stress leads to the accumulation of misfolded proteins in the ER lumen and the release of calcium into the cytosol, UPR activation helps to attenuate protein synthesis and to increase protein folding and degradation (Buytaert et al., 2013; Rao et al., 2004; Li et al., 2014; Hiramatsu et al., 2015). However, although UPR tries to restore ER homeostasis, an excessive stress or a failure to overcome the stress can lead to cell death. After PDT of Pc9-loaded CT26 cells, we found higher expression levels of several ER chaperones, such as GRP78/BIP, calnexin, Hsp90 and Hsp110. In addition, the release of $Ca^{2+}$ into the cytosol was partially blocked by the antioxidant TROLOX, suggesting that ROS are certainly affecting calcium storage. In this regard, it has been reported that the photo-oxidative damage to the ER $Ca^{2+}$-ATPase-2 (SERCA2) pump, an enzyme mediating the active transport of calcium from the cytosol to the ER, is associated to an increase of cytosolic $Ca^{2+}$ (Buytaert et al., 2006; Buytaert et al., 2007). It has also been reported that $Ca^{2+}$ mitochondrial uptake favors the increase of the inner mitochondrial membrane permeability, resulting in the release of apoptogenic factors into the cytosol (Orrenius et al., 2003). We found that higher levels of $Ca^{2+}$ contributed to cell death, as showed by the increment in cell

survival obtained in the presence of the chelator BAPTA-AM. We also presented evidence of the activation of the mitochondria-dependent pathway of apoptosis. Thus, our results indicate that an ER stress response participates in the apoptotic cell death caused after photodynamic treatment with Pc9-T1107. In the same way, apoptotic death caused by $Ca^{2+}$ disruption has been described for other photosensitizers mainly localized in the ER, such as hypericin (Buytaert et al., 2006) and ethylene glycol (EG)-porphyrin derivatives with EG chain in meta position (Moserova et al., 2012).

The higher cytosolic $Ca^{2+}$ concentrations found after photoactivation of Pc9 can also contribute to the activation of calpains (Buytaert et al., 2007; Moserova et al., 2012). The significant increase in cell survival observed after irradiation of Pc9-loaded cells pre-incubated with the calpains inhibitor PD 150606 certainly suggested a role of calpains in CT26 death. Furthermore, the almost full recovery of Bax expression levels obtained in the presence of PD 150606 indicated the involvement of calpains in Bax photodamage. In particular, the cleavage of the anti-apoptotic protein Bcl-2 by calpains after PDT has been previously described (Almeida et al., 2004; Buytaert et al., 2007; Oleinick et al., 2002). Although a calpain-dependent damage of the pro-apoptotic protein Bax after photodynamic treatment of cells has not yet been reported, it is possible to propose that calpains might contribute to Bax fragmentation to a more apoptotic fragment as showed in other apoptotic processes (Toyota et al., 2003).

## 5. Conclusions

In this work, we delineated the molecular signals leading to an apoptotic cell death after photoactivation of Pc9-loaded CT26 cells (Fig. 7). The generation of singlet oxygen and

other ROS in lysosomes and ER, the main sites of Pc9 intracellular localization, promotes the activation of a series of molecular targets. Permeabilization of lysosomal membranes leads to the release of proteases into the cytosol, contributing to Bid cleavage and caspase 8 activation. Pc9 photoactivation in the ER activates the UPR and increases calcium signaling, including the activation of calpains. The involvement of the mitochondrial apoptotic pathway was supported by the decrease of the mitochondrial membrane potential, the down-regulation of the anti-apoptotic Blc-2 proteins and the activation of caspase 9. The subsequent activation of caspase 3 occurs after mitochondrial damage, leading to PARP-1 cleavage and the resulting apoptotic cell death. Although these molecular signals converge to the induction of an apoptotic response, the contribution of other death modalities induced by PDT, such as necrosis, autophagy or a possible combination of these pathways can not be discarded.

## Conflict of interest

The authors declare no conflict of interest.

## Acknowledgments

This work was supported by grants from Consejo Nacional de Investigaciones Científicas y Técnicas (CONICET, PIP 0154: "Propiedades y mecanismo de acción de nuevos agentes antitumorales: péptidos quiméricos del IFN alfa, ftalocianinas de Zn(II) y derivados sintéticos de penicilinas"), Universidad de Buenos Aires (Programación Científica 2014-2017, UBACYT 20020130100024: "Mecanismos de acción de moléculas que intervienen en procesos que regulan la proliferación celular: rol de citoquinas y nuevos agentes antitumorales") and Agencia Nacional de Promoción Científica y Tecnológica (ANPCyT, PICT 0144: "Propiedades fotodinámicas de ftalocianinas de zinc (II) en un modelo de carcinoma de colon"), Argentina.

**References**

Almeida, R.D., Manadas, B.J., Carvalho, A.P., Duarte, C.B., 2004. Intracellular signaling mechanisms in photodynamic therapy. Biochim. Biophys. Acta 1704, 59–86. DOI: 10.1016/j.bbcan.2004.05.003

Appelqvist, H., Johansson, A.C., Linderoth, E., Johansson, U., Antonsson, B., Steinfeld, R., et al., 2012. Lysosome-mediated apoptosis is associated with cathepsin D-specific processing of bid at Phe24, Trp48, and Phe183. Ann. Clin. Lab. Sci. Summer 42 (3), 231-242

Aran, V., Victorino, A.P., Thuler, L.C., Ferreira, C.G., 2016. Colorectal Cancer: Epidemiology, Disease Mechanisms and Interventions to Reduce Onset and Mortality. Clin. Colorectal Cancer 15, 195-203. DOI: 10.1016/j.clcc.2016.02.008

Boya, P., Gonzalez-Polo, R.A., Poncet, D., Andreau, K., Vieira, H.L., Roumier, T., et al., 2003. Mitochondrial membrane permeabilization is a critical step of lysosome-initiated apoptosis induced by hydroxychloroquine. Oncogene 22, 3927-3936. DOI: 10.1038/sj.onc.1206622

Boya, P., Kroemer, G., 2008. Lysosomal membrane permeabilization in cell death. Oncogene 27, 6434-6451. DOI: 10.1038/onc.2008.310

Buytaert, E., Dewaele, M., Agostinis, P., 2007. Molecular effectors of multiple cell death pathways initiated by photodynamic therapy. Biochim. Biophys. Acta 1776 (1), 86-107. DOI: 10.1016/j.bbcan.2007.07.001

Buytaert, E., Callewaert, G., Hendrickx, N., Scorrano, L., Hartmann, D., Missiaen, L., et al., 2006. Role of endoplasmic reticulum depletion and multidomain proapoptotic BAX and BAK proteins in shaping cell death after hypericin-mediated photodynamic therapy. FASEB J. 20 (6), 756-758. DOI: 10.1096/fj.05-4305fje

Chiarante, N., García Vior, M.C., Awruch, J., Marino, J., Roguin, L.P., 2017. Phototoxic action of a zinc(II) phthalocyanine encapsulated into poloxamine polymeric micelles in 2D and 3D colon carcinoma cell cultures. J. Photochem. Photobiol. B 170, 140-151. DOI: 10.1016/j.jphotobiol.2017.04.009

Chiu, S.M., Xue, L.Y., Lam, M., Rodriguez, M.E., Zhang, P., Kenney, M.E., et al., 2010. A requirement for bid for induction of apoptosis by photodynamic therapy with a lysosome-but not a mitochondrion-targeted photosensitizer. Photochem. Photobiol. 86, 1161-1173. DOI: 10.1111/j.1751-1097.2010.00766.x

Cho, K., Yoon, S.Y., Choi, J.E., Kang, H.J., Jang, H.Y., Kim, D.H., 2013. CA-074Me, a Cathepsin B inhibitor, decreases APP accumulation and protects primary rat cortical neurons treated with okadaic acid. Neurosci. Lett. 548, 222-227. DOI: 10.1016/j.neulet.2013.05.056

Colussi, V.C., Feyes, D.K., Mulvihill, J.W., Li, Y.S., Kenney, M.E., Elmets, C.A., et al., 1999. Phthalocyanine 4 (Pc 4) photodynamic therapy of human OVCAR-3 tumor xenografts. Photochem. Photobiol. 69, 236-241. DOI: 10.1111/j.1751-1097.1999.tb03280.x

Conus, S., Perozzo, R., Reinheckel, T., Peters, C., Scapozza, L., Yousefi, S., et al., 2008 Caspase-8 is activated by Cathepsin D initiating neutrophil apoptosis during the resolution of inflammation. J. Exp. Med. 205 (3), 685-698. DOI: 10.1084/jem.20072152

Detty, M.R., Gibson, S.L., Wagner, S.J., 2004. Current clinical and preclinical photosensitizers for use in photodynamic therapy. J. Med. Chem. 47, 3897-3915. DOI: 10.1021/jm040074b

Dichiara, M., Prezzavento, O., Marrazzo, A., Pittalà, V., Salerno, L., Rescifina, A., et al., 2017. Recent advances in drug discovery of phototherapeutic non-porphyrinic anticancer agents. Eur. J. Med. Chem. 142, 459-485. DOI: 10.1016/j.ejmech.2017.08.070

Dobkowski, W.B., Murkin, J.M., 1998. A risk-benefit assessment of aprotinin in cardiac surgical procedures. Drug Saf. 18 (1), 21-41

Doleman, B., Mills, K.T., Lim, S., Zelhart, M.D., Gagliardi, G., 2016. Body mass index and colorectal cancer prognosis: a systematic review and meta-analysis. Tech. Coloproctol. 20, 517-535. DOI: 10.1007/s10151-016-1498-3

Dougherty, T.J., Gomer, C.J., Henderson, B.W., Jori, G., Kessel, D., Korbelik, M., et al., 1998. Photodynamic therapy. J. Natl. Cancer Inst. 90, 889-905

Doulias, P.T., Kotoglou, P., Tenopoulou, M., Keramisanou, D., Tzavaras, T., Brunk, U., et al., 2007. Involvement of heat shock protein-70 in the mechanism of hydrogen peroxide-induced DNA damage: the role of lysosomes and iron. Free Radic. Biol. Med. 42 (4), 567-577. DOI: 10.1016/j.freeradbiomed.2006.11.022

Droga-Mazovec, G., Bojic, L., Petelin, A., Ivanova, S., Romih, R., Repnik, U., et al., 2008. Cysteine cathepsins trigger caspase-dependent cell death through cleavage of bid and antiapoptotic Bcl-2 homologues. J. Biol. Chem. 283 (27), 19140-19150. DOI: 10.1074/jbc.M802513200

Fabris, C., Valduga, G., Miotto, G., Borsetto, L., Jori, G., Garbisa, S., et al., 2001. Photosensitization with zinc (II) phthalocyanine as a switch in the decision between apoptosis and necrosis. Cancer Res. 15, 7495-7500

Favoriti, P., Carbone, G., Greco, M., Pirozzi, F., Pirozzi, R.E., Corcione, F., 2016. Worldwide burden of colorectal cancer: a review. Updates Surg 68, 7-11. DOI: 10.1007/s13304-016-0359-y

Galluzzi, L., Vitale, I., Abrams, J.M., Alnemri, E.S., Baehrecke, E.H., Blagosklonny, M.V., et al., 2012. Molecular definitions of cell death subroutines: recommendations of the

Nomenclature Committee on Cell Death 2012. Cell Death Differ. 19, 107-120. DOI: 10.1038/cdd.2011.96

Guicciardi, M.E., Leist, M., Gores, G.J., 2004. Lysosomes in cell death. Oncogene 23, 2881-2890. DOI: 10.1038/sj.onc.1207512

Haggar, F.A., Boushey, R.P., 2009. Colorectal Cancer Epidemiology: Incidence, Mortality, Survival, and Risk Factors. Clin. Colon. Rectal Surg. 22, 191–1977. DOI: 10.1055/s-0029-1242458

Hassa, P.O., Hottiger, M.O., 2008. The diverse biological roles of mammalian PARPS, a small but powerful family of poly-ADP-ribose polymerases. Front. Biosci. 13, 3046-3082

Heinrich, M., Neumeyer, J., Jakob, M., Hallas, C., Tchikov, V., Winoto-Morbach, S., et al., 2004 Cathepsin D links TNF-induced acid sphingomyelinase to Bid-mediated caspase-9 and -3 activation. Cell Death Differ. 11, 550–563. DOI: 10.1038/sj.cdd.4401382

Hengartner, M.O., 2000. The biochemistry of apoptosis. Nature 407, 770-776. DOI: 10.1038/35037710

Hiramatsu, N., Chiang, W.C., Kurt, T.D., Sigurdson, C.J., Lin, J.H., 2015. Multiple Mechanisms of Unfolded Protein Response-Induced Cell Death. Am. J. Pathol. 185 (7), 1800-1808. DOI: 10.1016/j.ajpath.2015.03.009

Ichinose, S., Usuda, J., Hirata, T., Inoue, T., Ohtani, K., Maehara, S., et al., 2006. Lysosomal Cathepsin initiates apoptosis, which is regulated by photodamage to Bcl-2 at mitochondria in photodynamic therapy using a novel photosensitizer, ATX-s10 (Na). Int. J. Oncol. 29 (2), 349-355

Jancekova, B., Ondrouskova, E., Knopfova, L., Smarda, J., Benes, P., 2016. Enzymatically active Cathepsin D sensitizes breast carcinoma cells to TRAIL. Tumour Biol. 37, 10685-10696. DOI: 10.1007/s13277-016-4958-5

Johansson, A.C., Steen, H., Ollinger, K., Roberg, K., 2003. Cathepsin D mediates cytochrome c release and caspase activation in human fibroblast apoptosis induced by staurosporine. Cell Death Differ. 10, 1253-1259. DOI: 10.1038/sj.cdd.4401290

Johansson, A.C., Appelqvist, H., Nilsson, C., Kågedal, K., Roberg, K., Ollinger, K., 2010. Regulation of apoptosis-associated lysosomal membrane permeabilization. Apoptosis 15, 527-540. DOI: 10.1007/s10495-009-0452-5

Kågedal, K., Johansson, U., Ollinger, K., 2001. The lysosomal protease Cathepsin D mediates apoptosis induced by oxidative stress. FASEB J. 15, 1592-1594

Kaufmann, S.H., Hengartner, M.O., 2001. Programmed cell death: alive and well in the new millennium. Trends in Cell Biology 11, 526-534

Kolligs, F.T., 2016. Diagnostics and Epidemiology of Colorectal Cancer. Visc. Med. 32, 158-164. DOI: 10.1159/000446488

Kuzyniak, W., Ermilov, E.A., Atilla, D., Gürek, A.G., Nitzsche, B., Derkow, K., et al., 2016. Tetra-triethyleneoxysulfonyl substituted zinc phthalocyanine for photodynamic cancer therapy. Photodiagnosis Photodyn. Ther. 13, 148-157. DOI: 10.1016/j.pdpdt.2015.07.001

Li, H., Liu, C., Zeng, Y.P., Hao, Y.H., Huang, J.W., Yang, Z.Y., et al., 2016 Nanoceria-Mediated Drug Delivery for Targeted Photodynamic Therapy on Drug-Resistant Breast Cancer. ACS Appl. Mater. Interfaces 8, 31510-31523. DOI: 10.1021/acsami.6b07338

Li, Y., Guo, Y., Tang, J., Jiang, J., Chen, Z., 2014. New insights into the roles of CHOP-induced apoptosis in ER stress. Acta Biochim. Biophys. Sin. (Shanghai) 46 (8), 629-640. DOI: 10.1093/abbs/gmu048

Liaudet-Coopman, E., Beaujouin, M., Derocq, D., Garcia, M., Glondu-Lassis, M., Laurent-Matha, V., et al., 2006 Cathepsin D: newly discovered functions of a long-standing aspartic

protease in cancer and apoptosis. Cancer Lett. 237, 167-179. DOI: 10.1016/j.canlet.2005.06.007

Lin, C.F., Tsai, C.C., Huang, W.C., Wang, Y.C., Tseng, P.C., Tsai, T.T., et al., 2016. Glycogen Synthase Kinase-3β and Caspase-2 Mediate Ceramide- and Etoposide-Induced Apoptosis by Regulating the Lysosomal-Mitochondrial Axis. PLoS One 11 (1), e0145460. DOI: 10.1371/journal.pone.0145460

Liu, J., Zheng, L., Li, Y., Zhang, Z., Zhang, L., Shen, L., et al., 2015. Effect of DTPP-mediated photodynamic therapy on cell morphology, viability, cell cycle, and cytotoxicity in a murine lung adenocarcinoma cell line. Lasers Med. Sci. 30, 181-191. DOI: 10.1007/s10103-014-1637-x

Margaron, P., Grégoire, M.J., Scasnárt, V., Ali, H., van Lier, J.E., 1996. Structure-photodynamic activity relationships of a series of 4-substituted zinc phthalocyanines. Photochem. Photobiol. 63, 217-223

Marino, J., Garcia Vior, M.C., Dicelio, L.E., Roguin, L.P., Awruch, J., 2010. Photodynamic effects of isosteric water-soluble phthalocyanines on human nasopharynx KB carcinoma cells. Eur. J. Med. Chem. 45, 4129-4139. DOI: 10.1016/j.ejmech.2010.06.002

Marino, J., García Vior, M.C., Furmento, V., Blank, V., Awruch, J., Roguin, L.P., 2013. Lysosomal and mitochondrial permeabilization mediates zinc(II) cationic phtalocianine phototoxicity. Int. J. Biochem. Cell Biol. 45, 2553–2562. DOI: 10.1016/j.biocel.2013.08.012

Moserova, I., Kralova, J., 2012. Role of ER stress response in photodynamic therapy: ROS generated in different subcellular compartments trigger diverse cell death pathways. PLoS One 7 (3), e32972. DOI: 10.1371/journal.pone.0032972

Nylandsted, J., Gyrd-Hansen, M., Danielewicz, A., Fehrenbacher, N., Lademann, U., Høyer-Hansen, M., et al., 2004. Heat shock protein 70 promotes cell survival by inhibiting

lysosomal membrane permeabilization. J. Exp. Med. 200, 425-435. DOI: 10.1084/jem.20040531

O'Connor, A.E., Gallagher, W.M., Byrne, A.T., 2009. Porphyrin and nonporphyrin photosensitizers in oncology: preclinical and clinical advances in photodynamic therapy. Photochem. Photobiol. 85, 1053-1074. DOI: 10.1111/j.1751-1097.2009.00585.x

Oleinick, N.L., Morris, R.L., Belichenko, I., 2002. The role of apoptosis in response to photodynamic therapy: what, where, why, and how. Photochem. Photobiol. Sci. 1, 1-21

Orrenius, S., Zhivotovsky, B., Nicotera, P., 2003. Regulation of cell death: the calcium-apoptosis link. Nat. Rev. Mol. Cell. Biol. 4, 552–565

Patil, H., Saxena, S.G., Barrow, C.J., Kanwar, J.R., Kapat, A., Kanwar, R.K., 2017. Chasing the personalized medicine dream through biomarker validation in colorectal cancer. Drug Discov. Today 22 (1), 111-119. DOI: 10.1016/j.drudis.2016.09.022

Peters, D.C., Noble, S., 1999. Aprotinin: an update of its pharmacology and therapeutic use in open heart surgery and coronary artery bypass surgery. Drugs 57 (2), 233-260

Petersen, N.H., Kirkegaard, T., Olsen, O.D., Jäättelä, M., 2010. Connecting Hsp70, sphingolipid metabolism and lysosomal stability. Cell Cycle 9, 2305-2309. DOI: 10.4161/cc.9.12.12052

Pollack, J.R., Witt, R.C., Sugimoto, J.T., 2003. Differential effects of calpain inhibitors on hypertrophy of cardiomyocytes. Mol. Cell Biochem. 251 (1-2), 47-50

Rao, R.V., Ellerby, H.M., Bredesen, D.E., 2004. Coupling endoplasmic reticulum stress to the cell death program. Cell Death Differ. 11, 372–380. DOI: 10.1038/sj.cdd.4401761

Reiners, J.J.Jr., Caruso, J.A., Mathieu, P., Chelladurai, B., Yin, X.M., Kessel, D., 2002. Release of cytochrome c and activation of pro-caspase-9 following lysosomal photodamage involves Bid cleavage. Cell Death Differ. 9, 934-944. DOI: 10.1038/sj.cdd.4401048

Repnik, U., Stoka, V., Turk, V., Turk, B., 2012. Lysosomes and lysosomal Cathepsins in cell death. Biochim. Biophys. Acta 1824 (1), 22-33. DOI: 10.1016/j.bbapap.2011.08.016

Roberg, K., Johansson, U., Ollinger, K., 1999. Lysosomal release of Cathepsin D precedes relocation of cytochrome c and loss of mitochondrial transmembrane potential during apoptosis induced by oxidative stress. Free Radic. Biol. Med. 27, 1228-1237

Rodríguez-Hernández, A., Brea-Calvo, G., Fernández-Ayala, D.J., Cordero, M., Navas, P., Sánchez-Alcázar, J.A., 2006. Nuclear caspase-3 and caspase-7 activation, and poly(ADP-ribose) polymerase cleavage are early events in camptothecin-induced apoptosis. Apoptosis 11, 131-139. DOI: 10.1007/s10495-005-3276-y

Schröder, M., Kaufman, R.J., 2005. ER stress and the unfolded protein response. Mutat. Res. 569 (1-2), 29-63

Stoka, V., Turk, B., Schendel, S.L., Kim, T.H., Cirman, T., Snipas, S.J., et al., 2001. Lysosomal protease pathways to apoptosis. Cleavage of bid, not pro-caspases, is the most likely route. J. Biol. Chem. 276 (5), 3149-3157. DOI: 10.1074/jbc.M008944200

Szegezdi, E., Logue, S.E., Gorman, A.M., Samali, A., 2006. Mediators of endoplasmic reticulum stress-induced apoptosis. EMBO Rep. 7, 880-885

Taquet, J.P., Frochot, C., Manneville, V., Barberi-Heyob, M., 2007. Phthalocyanines Covantely Bound to Biomolecules for a Targeted Photodynamic Therapy. Curr. Med. Chem. 14, 1673-1687

Toyota, H., Yanase, N., Yoshimoto, T., Moriyama, M., Sudo, T., Mizuguchi, J., 2003. Calpain-induced Bax-cleavage product is a more potent inducer of apoptotic cell death than wild-type Bax. Cancer Lett. 189, 221-230

Vicente, M.G.H., 2001. Porphyrin-based sensitizers in the detection and treatment of cancer: recent progress. Curr. Med. Chem. Anti-Cancer Agents 1, 175-194

Victor, B.C., Anbalagan, A., Mohamed, M.M., Sloane, B.F., Cavallo-Medved, D., 2011. Inhibition of Cathepsin B activity attenuates extracellular matrix degradation and inflammatory breast cancer invasion. Breast Cancer Res. 13 (6), R115. DOI: 10.1186/bcr3058

Wang, H., Zhang, H.M., Yin, H.J., Wei, M.Q., Sha, H., Liu, T.J., et al., 2015. Combination of a novel photosensitizer DTPP with 650 nm laser results in efficient apoptosis, arresting cell cycle and cytoskeleton protein changes in lung cancer A549 cells. Lasers Med. Sci. 30, 77-82. DOI: 10.1007/s10103-014-1617-1

**Figure legends**

**Fig. 1.** Effect of Pc9-T1107 on cell cycle, the population of hypodiploid cells and caspases activities. 1 x $10^7$ CT26 cells were incubated for 24 h with or without 20 nM of Pc9-T1107 and then irradiated with a light dose of 2.8 J $cm^{-2}$. (A) Cell cycle phase distribution was assessed by flow cytometry as described in Materials and methods. Histograms from one representative experiment are shown (left panel). The analysis of DNA content in each phase was performed by excluding the sub $G_1$ cell population (right panel) and corresponds to mean values ± S.E.M. of three independent experiments. *$p < 0.05$, **$p < 0.005$, significantly different from control. (B) DNA content was determined by flow cytometry after PI staining. Histograms from one representative experiment show the percentage of hypodiploid cells from three different experiments (mean ± S.E.M., **$p< 0.005$). (C) Caspase 8 and 9 activities were measured at different times by using Z-IETD-AFC and Ac-LEHD-AMC substrates, respectively. Results were expressed as arbitrary fluorescence units corresponding to 100 µg of protein (mean ± S.E.M., n=3, *$p < 0.05$).

**Fig. 2.** Effect of photodynamic treatment with Pc9-T1107 on the expression levels of Bcl-2 family proteins, PARP-1 cleavage and mitochondrial transmembrane potential. CT26 cells were incubated for 24 h with or without 20 nM of Pc9-T1107 and then irradiated with a light dose of 2.8 J $cm^{-2}$. (A) After different times post-irradiation, cell lysates (50 µg) were submitted to Western blot assays. Results from one representative experiment are shown (upper panel). Densitometric analyses correspond to mean ± S.E.M. of three different experiments (lower panel). In the case of PARP-1, the quantification represents cleaved PARP-1 (89 kDa) with respect to full length PARP-1 (116 kDa). (B) Cells were incubated 0

h, 1 h or 3 h post-irradiation and then stained with 40 nM DiOC6(3) for 30 min. Control histogram corresponds to cells incubated without Pc9-T1107 at 0 h p.i. The decrease in $\Delta\Psi_m$ was determined by flow cytometry. Results represent the mean ± S.E.M., n =3. *p < 0.05, **p < 0.005 significantly different from control. #p < 0.05 significantly different from 0 h p.i. treated-cells.

**Fig. 3.** Lysosomal membrane permeabilization after Pc9-T1107 PDT. CT26 cells plated on coverslips were incubated with or without 20 nM Pc9-T1107 and irradiated in the absence (A) or presence (B) of 5 mM TROLOX. After photodynamic treatment, lysosomes were stained with 5 μM acridine orange and examined in a fluorescence microscope at different times p.i. (A) or at 1 h p.i. (B). Magnification 600 X (A, scale bar 50 μm) and 400 X (B, scale bar 75 μm). (C and D) CT26 cells exposed to 20 nM Pc9-T1107 were irradiated and incubated for different times. Cytosolic fractions (C) or whole cell lysates (D) were submitted to Western blot assays for Cathepsin D or Hsp70, respectively. Results from one representative experiment are shown. Densitometric analyses correspond to mean ± S.E.M., n =3, *p < 0.05, **p < 0.005 significantly different from control.

**Fig. 4.** Effect of proteases inhibitors on the phototoxic action triggered by Pc9-T1107. CT26 cells treated or not with 10 nM Pc9-T1107 were pre-incubated 1 h before irradiation with different concentrations of Pepstatin A (A), CA-074 Me (B) or aprotinin (C). 24 h after irradiation cell growth was determined by the MTT assay. Results are expressed as the percentage of cell survival with respect to that obtained in the absence of Pc9-T1107 (control). (D) After irradiation of 20 nM Pc9-T1107-loaded cells pre-incubated 1 h with 80 μM of Pepstatin A, caspase 8 activity was determined 1 h post-irradiation. (E) CT26 cells

loaded or not with 10 nM Pc9-T1107 were pre-incubated 1 h before irradiation with 80 μM of Pepstatin A. 1 h after irradiation cell lysates (50 μg) were submitted to Western blot. All data correspond to mean values ± S.E.M. of three different experiments, *$p < 0.05$, significantly different from control. #$p < 0.05$ significantly different from Pc9-treated cells.

**Fig. 5.** Endoplasmic reticulum stress. (A) CT26 cells were incubated with or without 20 nM of Pc9-T1107 and then irradiated with a light dose of 2.8 J $cm^{-2}$. At different times post-irradiation, cell lysates were submitted to Western blot assays. Results from one representative experiment are shown in the upper panel and densitometric analyses in the lower panel. (B) CT26 cells loaded with different concentrations of Pc9-T1107 were incubated with 2 μM of Fluo-4 AM for 30 minutes before being irradiated. Fluorescence intensity values were determined at different times post-irradiation with a microplate reader at 494 nm excitation and 516 nm emission wavelengths. (C) Cells were pre-incubated 1 h before irradiation with 5 mM of TROLOX and intracellular calcium measurement was performed at 3 h p.i. Results are expressed as the intensity of fluorescence with respect to that obtained in the absence of Pc9-T1107 at 3 h p.i. (control). (D) CT26 cells ($2 \times 10^4$ cells/well) loaded or not with 2 nM of Pc9-T1107 were pre-incubated for 1 h before light exposure with 5 μM of BAPTA-AM. Cell growth was determined 24 h after irradiation by the MTT assay. Results are expressed as the percentage of cell survival with respect to that obtained in the absence of Pc9-T1107 (control). All data correspond to mean values ± S.E.M. of three different experiments. *$p < 0.05$, **$p < 0.005$ significantly different from control, #$p < 0.05$, ##$p < 0.005$, significantly different from Pc9-treated cells.

**Fig. 6.** Effect of the calpain inhibitor PD 150606 on cell survival and Bax expression levels. (A) 2 x $10^4$ CT26 cells/well loaded or not with 2 nM of Pc9-T1107 were pre-incubated for 24 h before light exposure with different concentrations of PD 150606. Cell growth was determined 24 h after irradiation by the MTT assay. Results are expressed as the percentage of cell survival with respect to that obtained in the absence of Pc9-T1107 (mean ± S.E.M. of three different experiments). (B) CT26 cells treated or not with 10 nM Pc9-T1107 were pre-incubated 24 h before irradiation with a 100 μM concentration of PD 150606. 1 h after irradiation, cell lysates (50 μg) were submitted to Western blot. Results from one representative experiment are shown (upper panel). Densitometric analyses correspond to mean ± S.E.M., n =3 (lower panel). *$p < 0.05$, significantly different from control. #$p < 0.05$ significantly different from Pc9-treated cells.

**Fig. 7.** Proposed model of Pc9-induced cell death in CT26 cells. The generation of ROS induced after photodynamic treatment with Pc9-T1107 in lysosomes and ER cisterns leads to lysosomal membrane permeabilization, ER stress and activation of the mitochondrial pathway of apoptosis. The intracellular signals mediating the apoptotic response are indicated with solid lines. Dashed lines represent interactions reported by other authors.

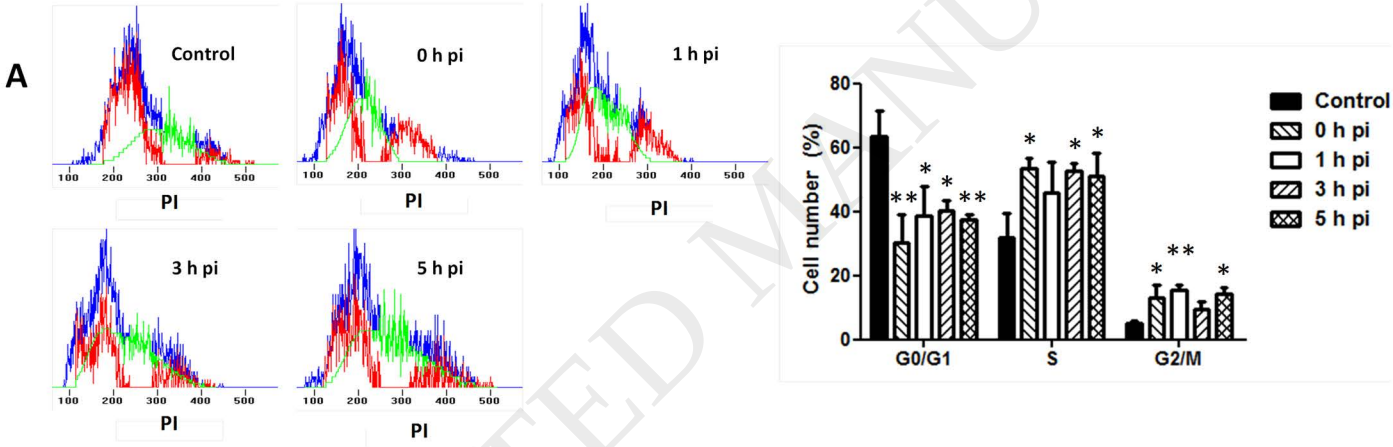


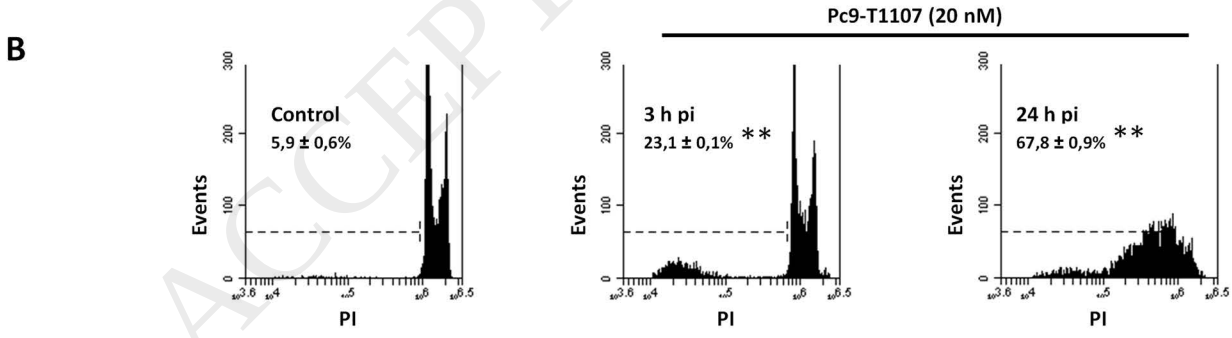


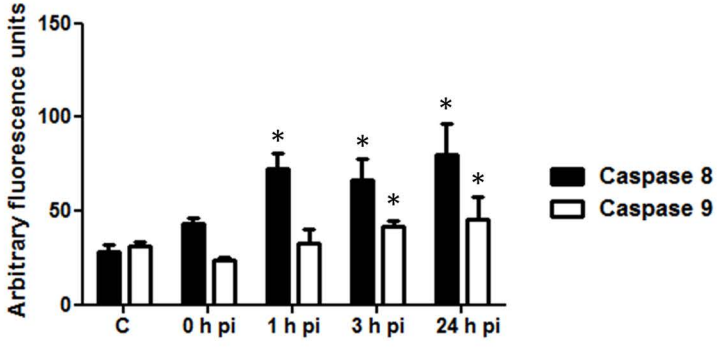

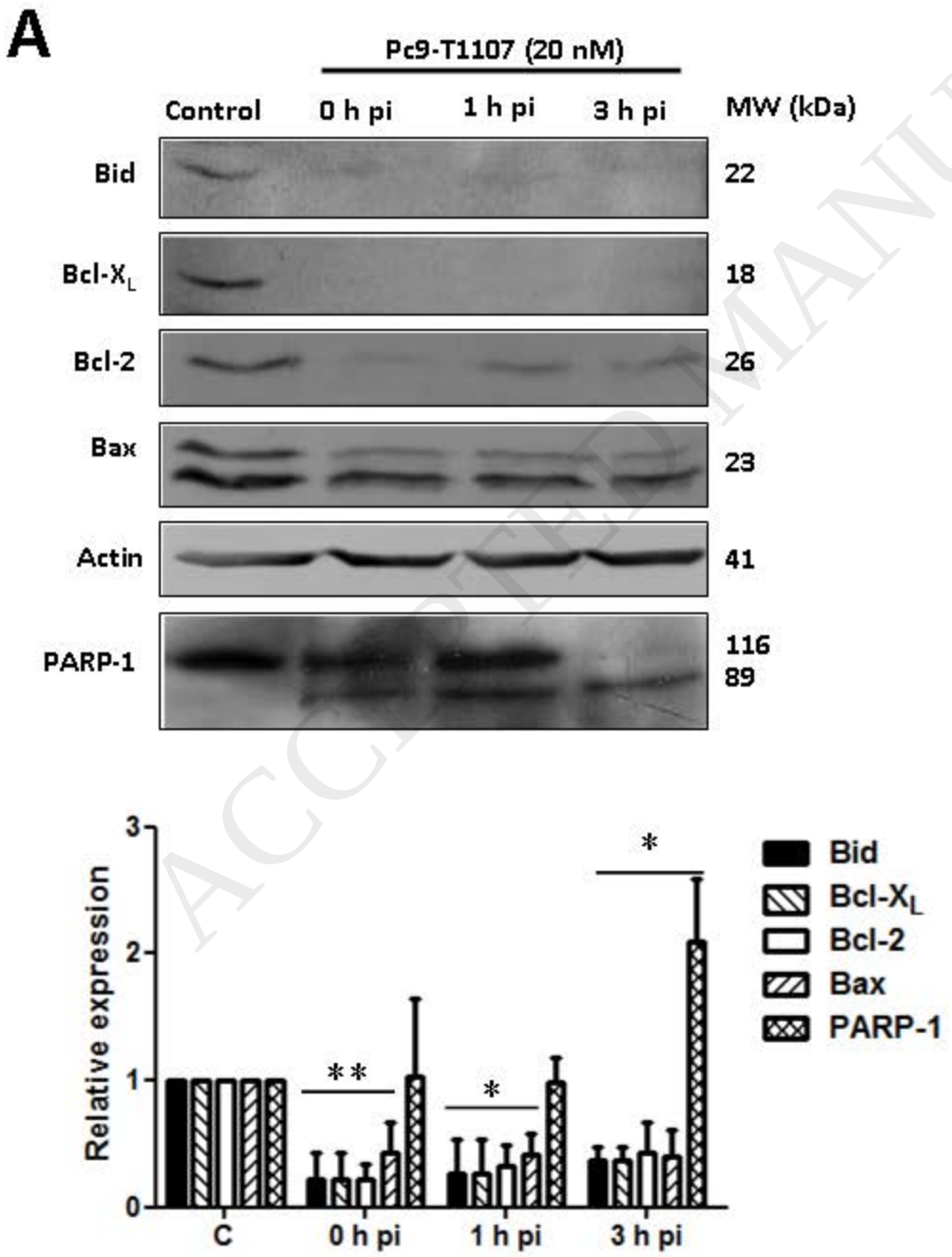


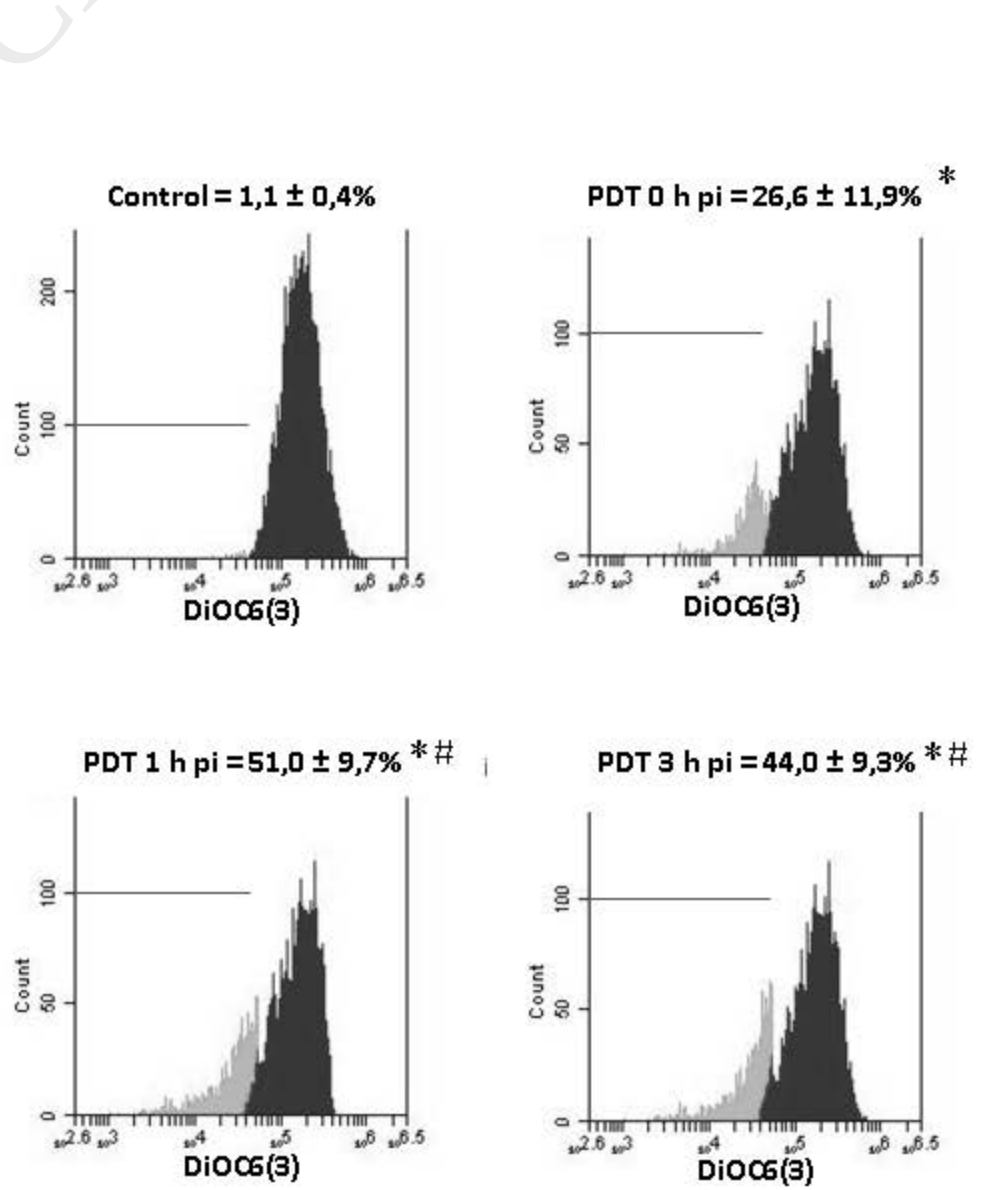

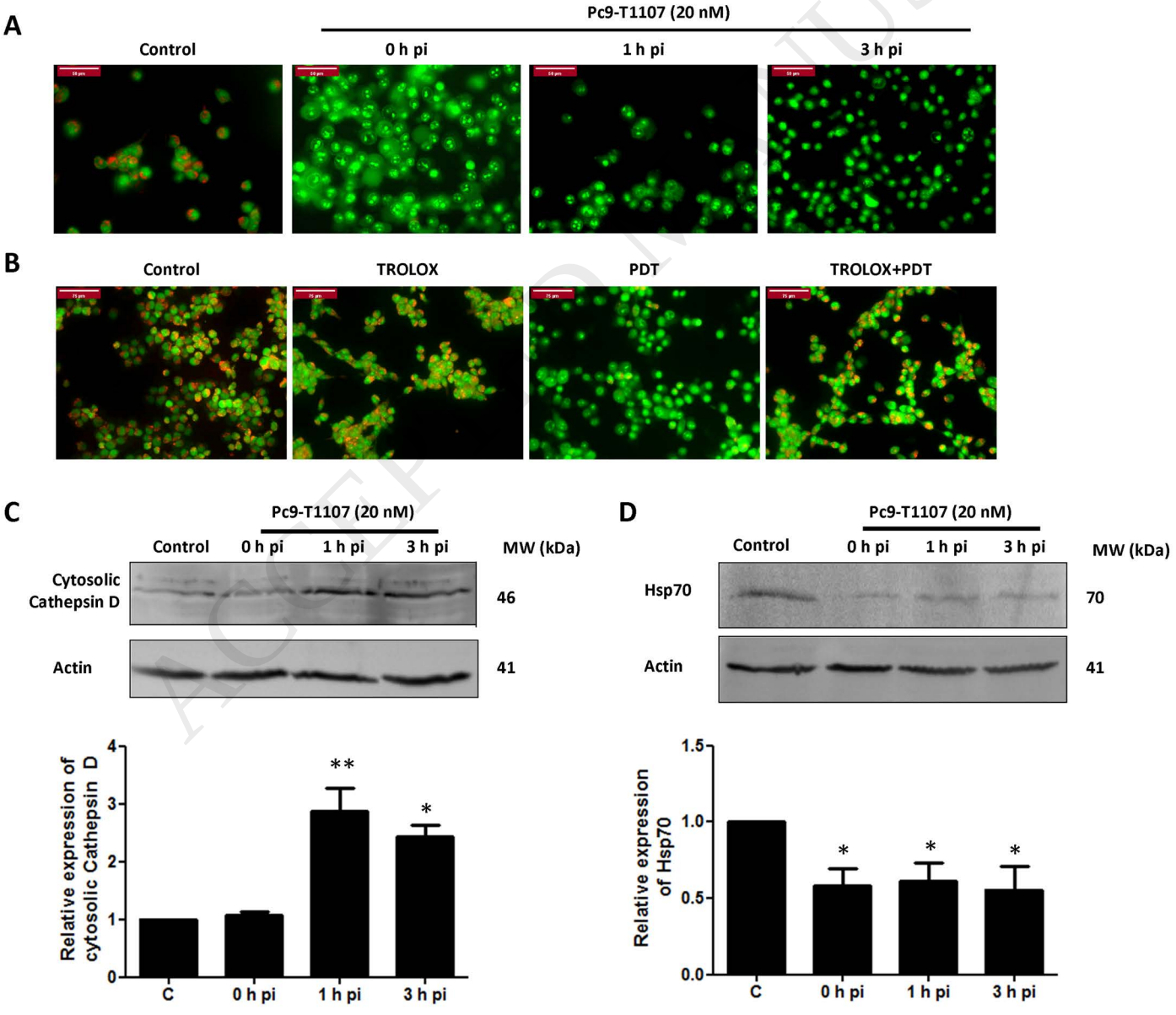
A
Pc9-T1107 (20 nM)
Control
0 h pi
1 h pi
3 h pi
B
Control
TROLOX
PDT
TROLOX+PDT
C
Pc9-T1107 (20 nM)
Control
0 h pi
1 h pi
3 h pi
MW (kDa)
Cytosolic Cathepsin D
46
Actin
41
Relative expression of cytosolic Cathepsin D
C
0 h pi
1 h pi
3 h pi
D
Pc9-T1107 (20 nM)
Control
0 h pi
1 h pi
3 h pi
MW (kDa)
Hsp70
70
Actin
41
Relative expression of Hsp70
C
0 h pi
1 h pi
3 h pi

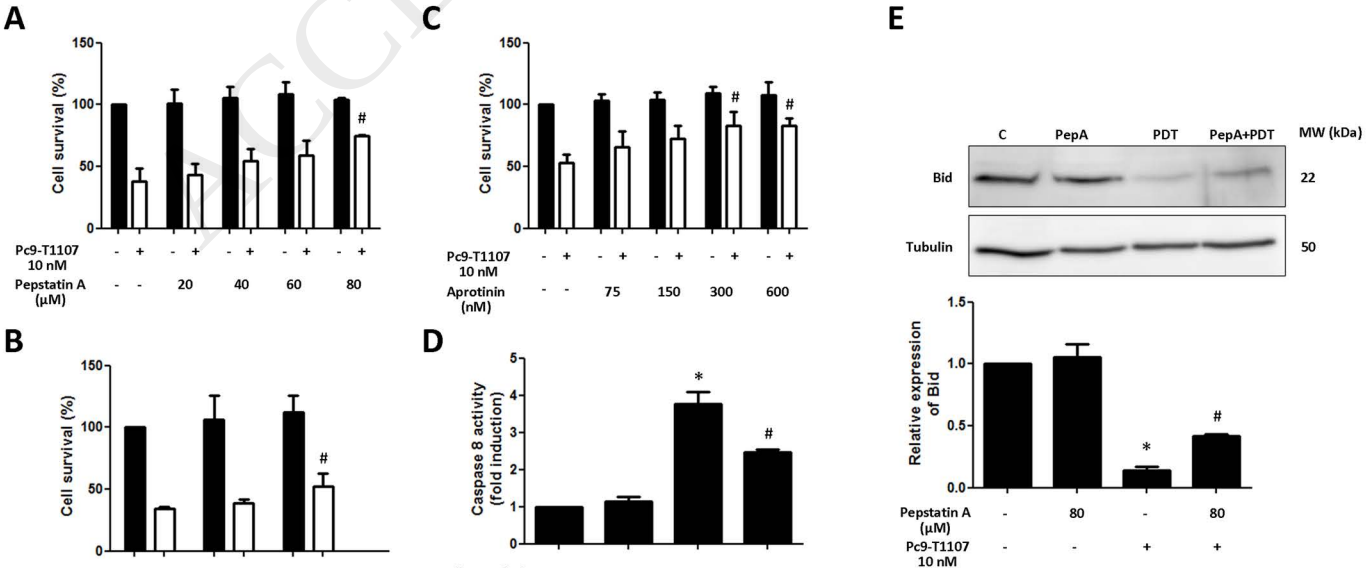
A
Cell survival (%)
150
100
50
0
#
Pc9-T1107 10 nM
- + - + - + - +
Pepstatin A (μM)
- - 20 40 60 80
B
Cell survival (%)
150
100
50
0
#
Pc9-T1107 10 nM
- + - + - +
CA-074 Me (μM)
- - 0.1 1.0
C
Cell survival (%)
150
100
50
0
#
#
Pc9-T1107 10 nM
- + - + - + - + - +
Aprotinin (nM)
- - 75 150 300 600
D
Caspase 8 activity (fold induction)
5
4
3
2
1
0
*
#
Pepstatin A (μM)
- 80 - 80
Pc9-T1107 20 nM
- - + +
E
C
PepA
PDT
PepA+PDT
MW (kDa)
Bid
22
Tubulin
50
Relative expression of Bid
1.5
1.0
0.5
0.0
*
#
Pepstatin A (μM)
- 80 - 80
Pc9-T1107 10 nM
- - + +

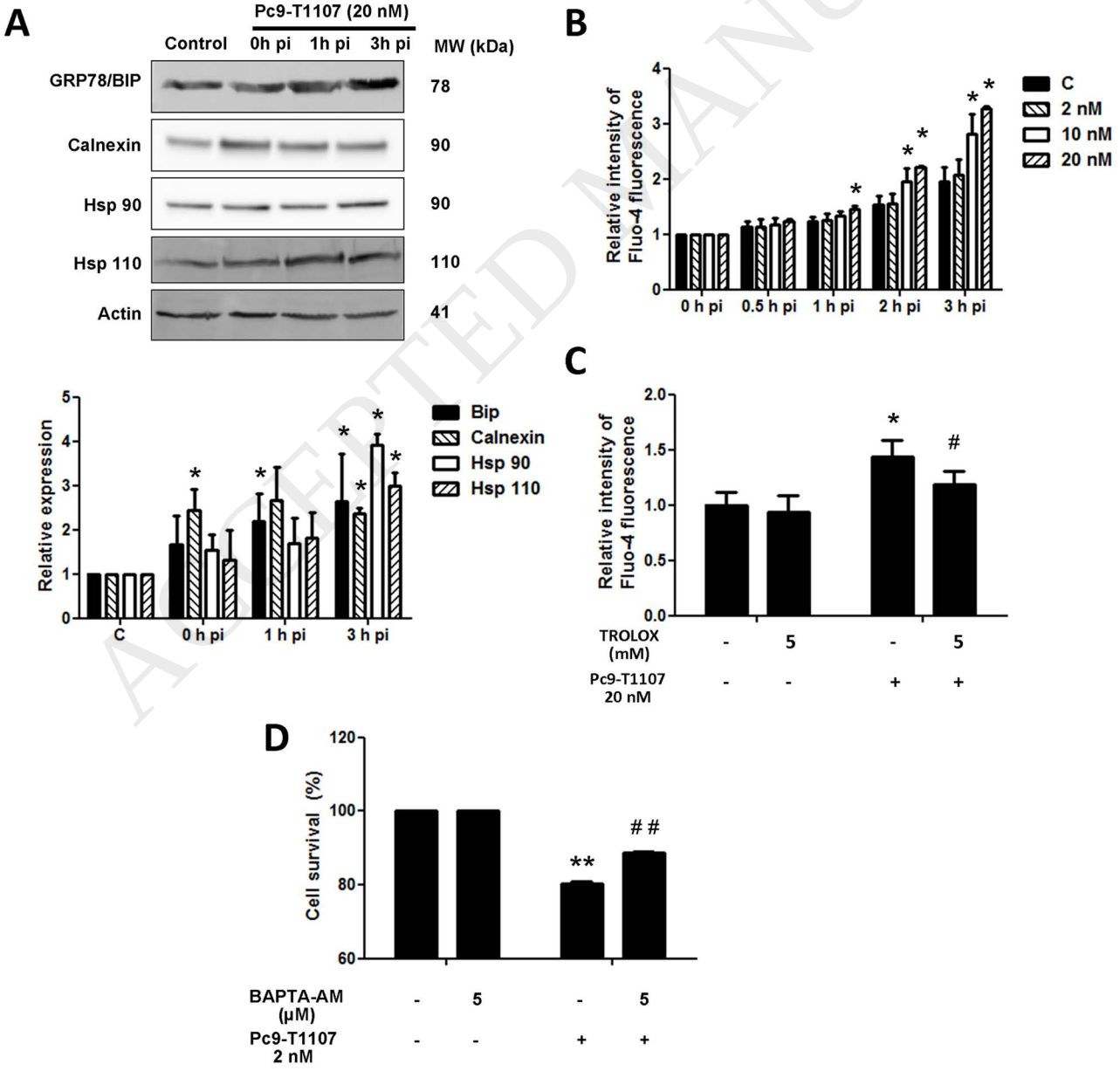

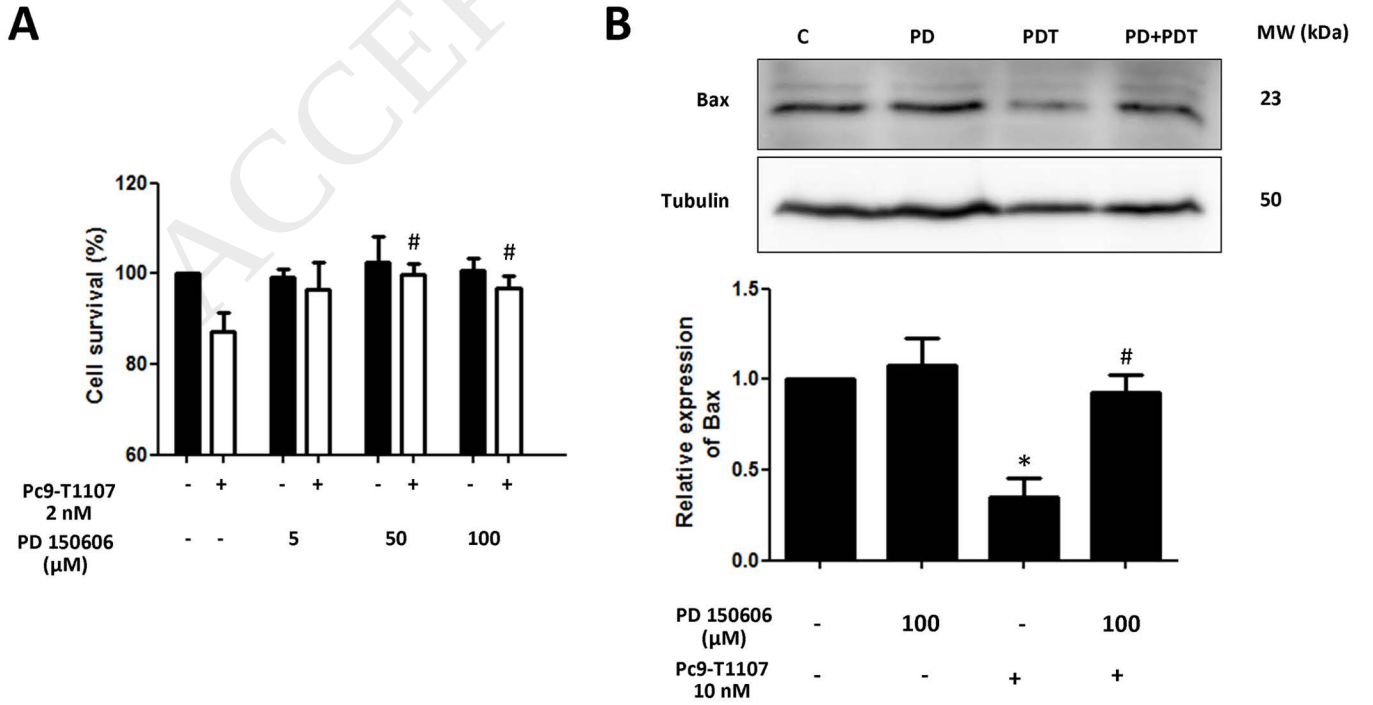
A
120
100
80
60
Cell survival (%)
#
#
Pc9-T1107
2 nM
PD 150606
(μM)
- + - + - + - +
- - 5 50 100
B
C
PD
PDT
PD+PDT
MW (kDa)
Bax
23
Tubulin
50
1.5
1.0
0.5
0.0
Relative expression
of Bax
*
#
PD 150606
(μM)
- 100 - 100
Pc9-T1107
10 nM
- - + +

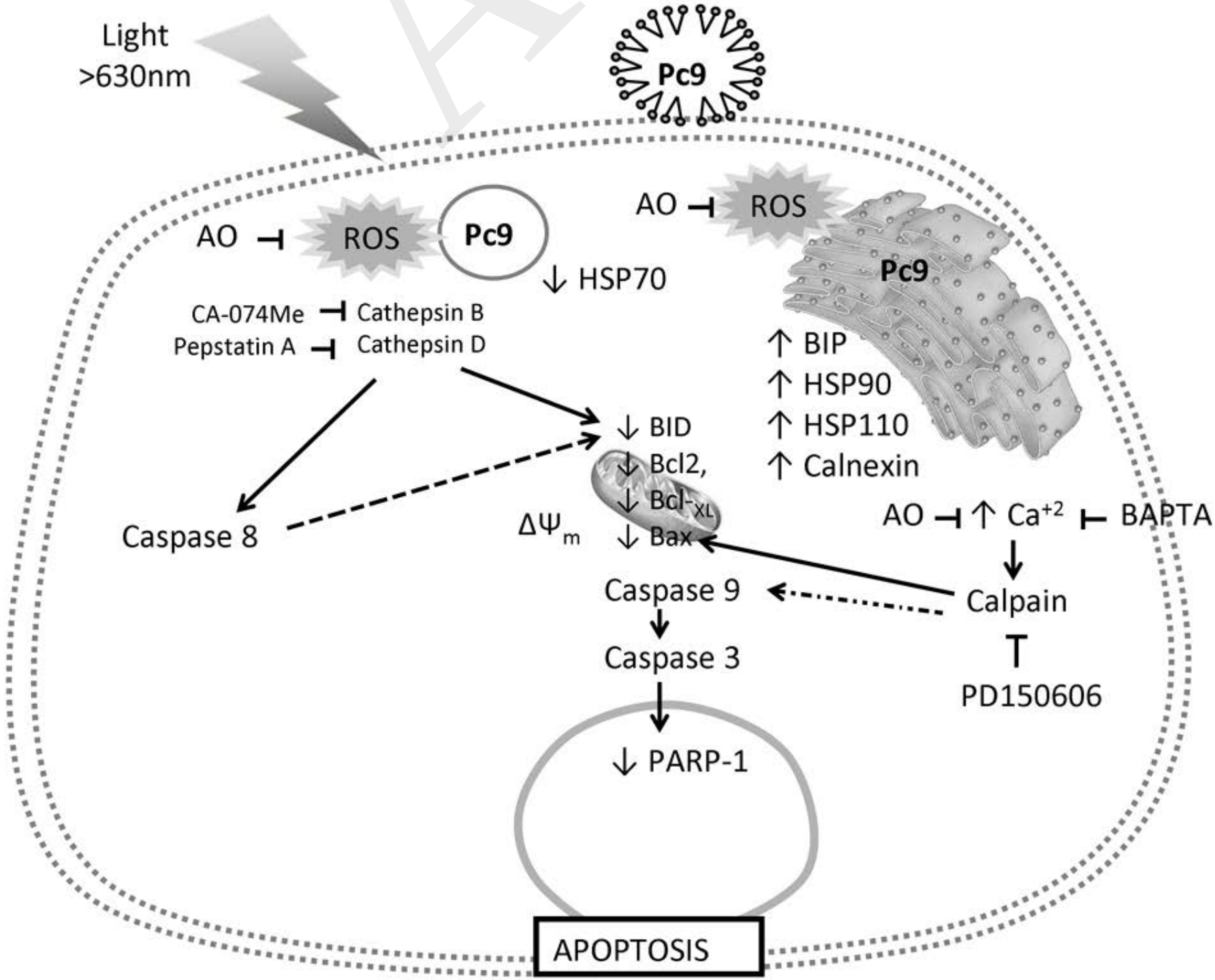
Light
>630nm
Pc9
AO
ROS
Pc9
↓ HSP70
CA-074Me
Cathepsin B
Pepstatin A
Cathepsin D
AO
ROS
Pc9
↑ BIP
↑ HSP90
↑ HSP110
↑ Calnexin
↓ BID
↓ Bcl2,
↓ Bcl-xL
↓ Bax
ΔΨm
Caspase 8
AO
↑ Ca+2
BAPTA
Calpain
PD150606
Caspase 9
Caspase 3
↓ PARP-1
APOPTOSIS